Hydrogen-mediated creation and annihilation of strain in amorphous silicon

N. H. Nickel and W. B. Jackson
Xerox Palo Alto Research Center, 3333 Coyote Hill Road, Palo Alto, California 94304
(Received 3 August 1994)

The influence of an increasing hydrogen concentration on the properties of hydrogenated amorphous silicon (a-Si:H) was investigated. An increase of the Si-H bond concentration by as much as 3×10^{21} cm^{-3} changes neither the defect density, the weak-bond density, nor the metastability. These results suggest that hydrogen is accommodated in pairs pinning the hydrogen chemical potential, which is indicative of a negative correlation energy. Data on annealing of a-Si:H at high temperatures show that the exponential band tails do not broaden as a function of the temperature. These experiments suggest that the random-network strain energy in device-quality a-Si:H is in metastable equilibrium. Based on our experimental results, we propose that internal strain propagates within the network and can be generated or reduced by annealing and/or the incorporation of hydrogen. According to maximum entropy the slope of the exponential band tails represents the average strain energy per lattice bond.

I. INTRODUCTION

Despite the successful incorporation of hydrogenated amorphous silicon (a-Si:H) as an active layer in thin-film transistors and photovoltaic devices, metastability remains a problem. Indirect evidence suggests that hydrogen participates in the defect creation mechanism by stabilizing newly created Si dangling bonds.[1] Recently, the observation of light-induced defect creation in hydrogenated polycrystalline silicon has clearly demonstrated the participation of H in this phenomenon. Unlike in a-Si:H, the magnitude of light-induced degradation decreases with repeated annealing and illumination cycles. However, the metastability can be rejuvenated simply by reexposing poly-Si:H to monatomic hydrogen.[2] Because of the similarity of amorphous and poly-Si metastable phenomena, it is highly likely that H is involved in metastability in a-Si:H.

In addition to the role of hydrogen, metastability also involves strained or weak Si-Si bonds which are converted to Si-H and dangling bonds by H. The characteristic exponential band tails observed in amorphous silicon are attributed to the localized states of strained Si-Si bonds. In order to further understand metastability, one would have to vary the strained Si-Si bonds independently of the H concentration.

Typically, this has been accomplished through variation of deposition conditions. A variety of deposition techniques has been used to minimize strain and ultimately grow stable amorphous silicon. In one approach high deposition temperatures have been suggested, and the observed reduction of the light-induced defect creation in the resulting films was attributed to a decrease of the hydrogen content from 10 to 4 at. %.[3] In another approach a-Si:H films were deposited in a remote hydrogen-plasma reactor at 400 °C. The material exhibited an improved thermal stability, although the hydrogen content was maintained at 10 at. % by H dilution.[4] The improved stability of the a-Si:H films was attributed to a change in the H migration kinetics and to structural changes in the random silicon-hydrogen network. Presumably, at high temperatures H is incorporated in more stable configurations, and the density of weak Si-Si bonds may be reduced.[4] The effects of hydrogen introduced during film growth on the equilibrium defect density, metastability, and Si-Si bond disorder have been widely studied. A variation of the H concentration commonly is achieved by changing deposition parameters such as temperature and power or by H dilution. Unfortunately in all cases, changing the deposition conditions alters the Si network and the H bonding simultaneously, so one cannot separate the two factors effectively.

In this paper posthydrogenation is used to increase the H concentration after sample deposition while maintaining a roughly fixed Si network. Furthermore, posthydrogenation enables us to obtain information for various H concentrations by characterizing the specimens between individual exposures. We find that an increase of the Si-H bond density by up to 3×10^{21} cm^{-3} does not alter the defect density in the annealed state, change the Urbach tail, nor alter metastable defect creation. High-temperature anneals of device-grade a-Si:H and subsequent rapid thermal quenching also does not influence the defect density or the Urbach tail. These observations are discussed in terms of a metastable equilibrium of network strain. It is proposed that the exponential band tails of strained Si-Si bonds occur because the remaining strain is distributed according to maximum entropy.

This paper is organized as follows. In the experimental part (Sec. II) we describe sample preparation and the experimental techniques used to obtain the data. In Sec. III the results are presented, and in Sec. IV we discuss the implications of the results for hydrogen bonding. Our data support a hydrogen-cluster model in which H is trapped or released from H clusters which nucleate and grow in response to added hydrogen. Adding H removes strain energy until an equilibrium between strain creation and reduction is reached. The residual strain is partitioned among the various Si-Si bonds according to maximum entropy, giving rise to exponential band tails. The

 ©1995 The American Physical Society

exponential Urbach slope represents the average energy per network bond.

II. EXPERIMENT

A. Samples

Hydrogenated amorphous silicon films were deposited on quartz substrates by silane decomposition in a rf-glow discharge at 230 °C. Some of the quartz substrates contained patterned chromium contacts. The *a*-Si:H films were grown to thicknesses of 0.25 and 1 μm under conditions known to give high quality nominally undoped material with a dark conductivity of $\sigma_d \approx 10^{-9}\ \Omega^{-1}\,\mathrm{cm}^{-1}$. Electrical contact to the Cr layers was established by opening holes in the *a*-Si:H film.

The postdeuteration procedure of the samples consisted of the following steps. Prior to deuteration, the samples were given a metal-oxide-semiconductor grade detergent cleaning, a deionized water rinse, a 10-s dip in dilute 20:1 HF water mixture, a second deionized water rinse, and were dried using dry N_2. These steps remove any oxide layer which might act as a barrier for deuterium incorporation. Then the samples were exposed to an optically isolated remote deuterium plasma. The microwave power was held to 70 W at 2.45 GHz. The gas pressure was 2 Torr and the D flow rate was 50 SCCM (SCCM denotes cubic centimeter per minute at STP). The samples were deuterated through a sequence of 1-h exposures at 350 °C. To avoid the outdiffusion of a significant amount of hydrogen during the heating period, the plasma was ignited at 150 °C. After 60-min exposure at 350 °C the samples were slowly cooled down to room temperature to avoid a quench-in of additional dangling-bond defects,[5] and the plasma was turned off at 70 °C.

B. Measurements

A number of measurement techniques were employed to determine various properties of the films. The concentration profiles of H and D were measured simultaneously by secondary-ion-mass spectrometry (SIMS) using a Cs^+ ion beam. The hydrogen and deuterium concentrations were calibrated using a standard crystalline silicon sample with a hydrogen implantation dose of 1×10^{14} cm^{-2}. The absolute concentration values are accurate to within a factor of 2, but the relative precision when comparing two profiles is much better. The depth scales were obtained by measuring the depth of the sputtered craters.

A standard hydrogen evolution experiment was performed on 1-μm-thick *a*-Si:H flakes which were obtained by depositing *a*-Si:H on aluminum foil and then lifting the *a*-Si:H film off the substrate. The volume was determined by weighting the flakes. As the temperature was increased up to 1000 °C with a rate of 20 ° C/min, the flux of evolving of H_2 was measured.

On some samples the room-temperature dark conductivity, the photoconductivity at $h\nu=2.0$ eV, the defect density N_D, and the Urbach slope were measured in the annealed state *A*, after each postdeuteration sequence and again after an intense exposure to white light (5 $\mathrm{W\,cm}^{-2}$) for 15.5 h. The Urbach slope was measured using the constant-photocurrent method (CPM). The illuminations were performed at 300 K with water-filtered light from a xenon arc lamp. Care was taken to minimize and evaluate sample heating from light absorption. The samples were mounted on a copper block in a chamber providing convective cooling. A thermal conductive paste was used to minimize temperature gradients between the specimens and the sample holder.

Finally, a set of *a*-Si:H films was annealed at high temperatures ranging from 450 to 550 °C. To avoid explosive H outdiffusion which would destroy the specimens, annealing was performed in the presence of monatomic H generated in a remote plasma. A significant loss of hydrogen at the substrate/sample interface was avoided by depositing the *a*-Si:H film on top of an *a*-Si:N_x:H buffer layer. The nitride serves as a source of H keeping the back interface hydrogenated. The samples were then quenched with a cooling rate of 10 °C/s. Before and after annealing the films were characterized by measurements of the defect density and Urbach tail.

III. RESULTS

A. Hydrogen and deuterium depth profiles

Typical concentration profiles for hydrogen, deuterium, and the total concentration of hydrogen plus deuterium, are shown in Fig. 1. The *a*-Si:H films were exposed to monatomic D for 1 and 8 h, respectively. During postdeuteration the concentration of atomic D in the plasma is constant and was estimated to be about 10^{15} cm^{-3} using electron-spin-resonance (ESR) measurements of atomic H or D.[6] At the sample surface (depth = 0) hydrogen is displaced by deuterium. With increasing exposure time t_d, the H displacement advances toward the interface indicated by the peaks in the concentration profiles [Fig. 1(b)]. The H loss at the surface is about one order of magnitude. Despite the H outdiffusion, the total concentration of hydrogen plus deuterium increases from 5×10^{21} to 8×10^{21} cm^{-3} after a total exposure of 8 h to monatomic D. The loss of H due to outdiffusion is overcompensated for by the incorporation of D from the remote plasma, and a net increase of the hydrogen plus deuterium concentration of 3×10^{21} cm^{-3} is observed. At such high concentrations the effective diffusion coefficient is concentration independent, and the diffusion profile can be described by a complementary error function (erfc). The diffusion length is related to the diffusion time t_d by $x_0=(4D_{\mathrm{eff}}t_d)^{1/2}$.[7] The diffusion length is determined from (i) the distance where the hydrogen concentration decreases to 16% of the bulk value or (ii) the distance where the deuterium concentration decreases to 16% of the surface concentration. From both the H outdiffusion and the D indiffusion, the diffusion length is approximately the same ($x_0 \approx 46$ nm). Therefore, a diffusion coefficient of $D_{\mathrm{eff}}=1.5\times10^{-15}$ cm^{-2}/s is obtained for both H and D [Fig. 1(a)].

Structural information on the incorporated deuterium can be obtained by Raman-backscattering measurements. With increasing deuteration time the Si-H stretching vi-

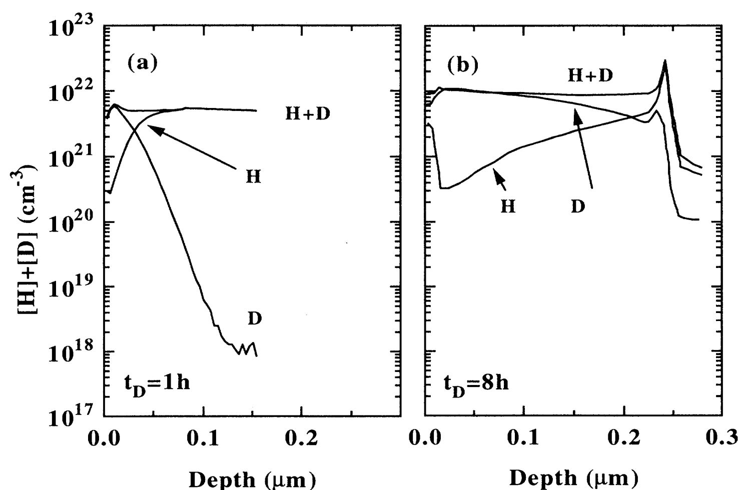

FIG. 1. Hydrogen and deuterium depth profiles of a-Si:H films obtained after an exposure to monatomic deuterium at 350 °C for (a) 1 and (b) 8 h, respectively. The concentration profiles for H and D were measured simultaneously. The peaks in the depth profiles indicate the interface to the substrate.

bration at $\omega_{\text{Si-H}}=2010\ \text{cm}^{-1}$ decreases while the Si-D stretching vibration at $\omega_{\text{Si-D}}=1470\ \text{cm}^{-1}$ increases. The integrated intensity of the Si-H and Si-D Raman lines shows that (i) deuterium completely substitutes for hydrogen and (ii) the total number of Si-H plus Si-D bonds increases in proportion to the total H plus D concentration,[8] which is in good agreement with the SIMS results of Fig. 1. Using estimates of the Raman cross sections, it can be inferred that most of the added D and H is incorporated as Si-D and Si-H rather than as molecular D_2, H_2, or HD. The incorporation of deuterium as an interstitial molecular species is unlikely, since neither Raman nor nuclear-magnetic-resonance measurements have detected large quantities in annealed samples or single crystal silicon.[9] Consequently, the exposure of a-Si:H films to monatomic deuterium for 8 h at $T_H=350\,^{\circ}\text{C}$ increases the concentration of Si-H plus Si-D bonds by $3\times10^{21}\ \text{cm}^{-3}$. This result should have a direct impact upon the metastability and the electrical and optical properties of a-Si:H.

B. Metastability

The incorporation of hydrogen in amorphous semiconductors is known to change the optical band gap E_g. It has been shown that the optical gap of unhydrogenated a-Si sputtered at 300 °C increases with increasing H content.[10,11] Since postdeuteration increased the total hydrogen plus deuterium concentration from 5×10^{21} to $8\times10^{21}\ \text{cm}^{-3}$, one would anticipate an increased optical band gap. From optical-transmission measurements the Tauc gap of a-Si:H films was determined after film preparation and after 8-h exposure to monatomic deuterium. The increase of the total Si-H/Si-D bond density by $3\times10^{21}\ \text{cm}^{-3}$ caused the Tauc gap to increase by only 4 meV. Similar small changes of E_g with increasing H content have been observed in *in situ* spectroscopic ellipsometry measurements.[12] This result is consistent with measurements showing that most of the increase of the optical gap due to an increase of the H concentration depends on the H concentration during film deposition, and occurs for low H concentrations.

CPM spectra measured in the annealed state A and after intense light soaking with white light for 15.5 h are plotted in Fig. 2. The unexposed a-Si:H film is represented by the solid curves. The dashed and dotted curves were obtained on a specimen exposed to monatomic D for 3 and 6 h, respectively. Since the increase of the optical band gap due to an increase of the total H plus D concentration is small and within the error bars of the CPM spectra, the normalized spectra of the postdeuterated specimens were adjusted to the band-tail region of the unexposed a-Si:H film (solid curves in Fig. 2). The saturated CPM signal of the postdeuterated films increased by a factor of 2 at $h\nu=2.0$ eV with respect to the unexposed a-Si:H film presumably due to a change of the surface band bending in the a-Si:H film, as discussed further below.

Normalization of the CPM spectra reveals an important result. The CPM spectra obtained in both the annealed state and the light-soaked state are basically unaffected by the postdeuteration. The increase of the total H plus D concentration by up to $3\times10^{21}\ \text{cm}^{-3}$

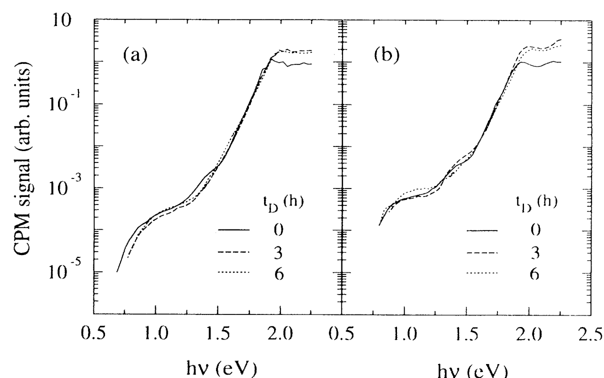

FIG. 2. Normalized CPM spectra of a-Si:H samples measured at 300 K. The spectra were taken before and after exposure to monatomic deuterium for 3 and 6 h, respectively. (a) State A; (b) after intense light soaking with white light ($P=5$ W cm^{-2}).

changed neither the defect region ($h\nu = 0.8-1.3$ eV) nor the Urbach tail significantly. Several important conclusions can be drawn from this observation. The additional deuterium introduced from a remote D plasma does not (i) increase the defect density in the annealed state [Fig. 2(a)], (ii) passivate preexisting dangling-bond defects, (iii) decrease the concentration of weak Si-Si bonds, nor (iv) stabilize the amorphous network. The last conclusion was reached from the observation that prolonged exposure to intense white light always increased the defect density by a factor of 3 independent of the total H plus D concentration [Figs. 2(b) and 3(a)]. The light-induced increase of the defect density, ΔN_D, was determined by taking the ratio of the CPM spectra in the annealed state and after light soaking. Figure 3(a) displays ΔN_D versus the deuteration time t_d. Prolonged illumination generates 5×10^{16} cm^{-3} defect states independent of the total H plus D concentration.

After each deuteration sequence the conductivity activation $E_C - E_F$, where E_C and E_F are the energies of the conduction band and Fermi level, respectively, was determined in the annealed state A and after prolonged illumination. In Fig. 3(b) $E_C - E_F$ is plotted as a function of the deuteration time t_d. The open triangles represent state A, and the full triangles were obtained in the light-soaked state B. The activation energy of the unexposed film ($E_C - E_F = 0.56$ eV) is smaller than in thick intrinsic a-Si:H films. In thin a-Si:H films the influence of the surface band bending upon $E_C - E_F$ is more pronounced than in thick films, resulting in a net decrease of $E_C - E_F$. Postdeuteration for $t_d = 2h$ increases the activation energy by about 0.1 eV. Since exposure to monatomic deuterium does not alter dopant or impurity concentrations,

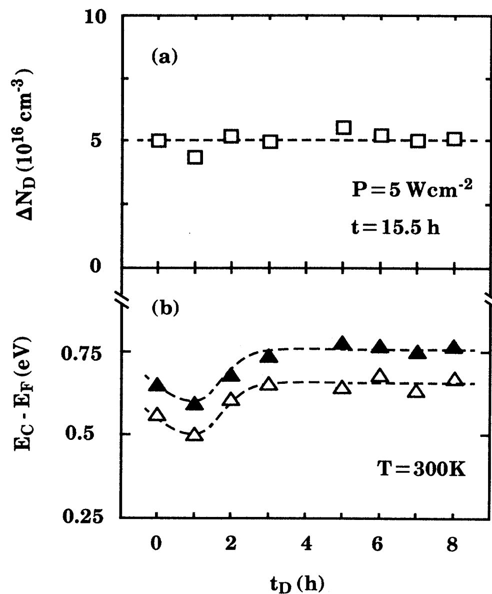

FIG. 3. (a) Density of created dangling-bond defects after prolonged illumination with white light at 300 K as a function of the plasma exposure time t_d ($P = 5$ W cm^{-2}, $t = 15.5$ h). (b) Fermi energy in the annealed state A (open triangles) and in the light-soaked state B (full triangles) vs deuteration time.

the increase of $E_C - E_F$ is most likely caused by a reduction of the surface band bending. This observation supports the previous result of Fig. 2, where the CPM absorption curves obtained on postdeuterated a-Si:H films exhibited an increase of the CPM signal at $h\nu \geq 2$ eV. Light-induced defect creation causes the Fermi energy to increase by approximately 0.1 eV independent of the exposure time, and thus the total H plus D concentration of the a-Si:H film. Furthermore, $E_C - E_F$ in state B (full triangles) reveals the same dependence on the exposure time as in state A (open triangles). This is consistent with the observation that the generation of metastable defects is independent of the H concentration.

C. Annealing at high temperatures

An increase of the total Si-H bond density by 3×10^{21} cm^{-3} affected neither the electrical nor the optical properties of amorphous silicon. In particular the Urbach tail, which commonly is believed to represent the density of weak Si-Si bonds, did not change with increasing H concentration even though one would expect that it is energetically favorable for H to remove weak Si-Si bonds. This suggests that the density and distribution of weak Si-Si bonds is in some sort of dynamic steady state with the strong Si-Si bonds during the formation and rupture of Si-H bonds. If this steady state between strong and weak bonds is a thermal equilibrium process, one would expect that the weak-bond–strong-bond conversation process depends on temperature.

The temperature dependence of the weak-bond–strong-bond steady state was investigated by annealing a-Si:H at temperatures close to 600 °C, at which a-Si:H crystallizes with a crystallization velocity of $\approx 10^{-7}$ cm/s.[13] In order to keep the hydrogen concentration of the samples constant during the anneals, the specimens were exposed to monatomic hydrogen. Subsequently the specimens were rapidly cooled to room temperature with a cooling rate of 10 °C/s while the plasma remained on. Since the crystallization velocity is thermally activated with 2.7 eV,[14] one would expect that this procedure freezes in the high-temperature equilibrium concentrations of weak and strong Si-Si bonds. In case of a thermal equilibrium reaction with a nonzero enthalpy of reaction, the weak Si-Si bond density and, consequently, the Urbach energy should change.

In these measurements undoped a-Si:H films were annealed at 450 and 550 °C for 1 h, respectively, to provide enough time for the amorphous network to equilibrate, and then thermally quenched with a cooling rate of 10 °C/s. A significant loss of hydrogen during the anneals was prevented by exposing the sample to monatomic hydrogen and depositing a thin hydrogen-rich a-SiN$_x$:H layer on the substrate prior to the a-Si:H deposition. The silicon nitride layer serves as a solid source of H to help maintain the H concentration of the sample/substrate interface and as a diffusion barrier to reduce evolution of H into the substrate. SIMS depth profiles of the hydrogen concentration are shown in Fig. 4. The as-deposited sample is represented by the solid curve, and exhibits a constant H concentration of 7×10^{21} cm^{-3}. The dashed

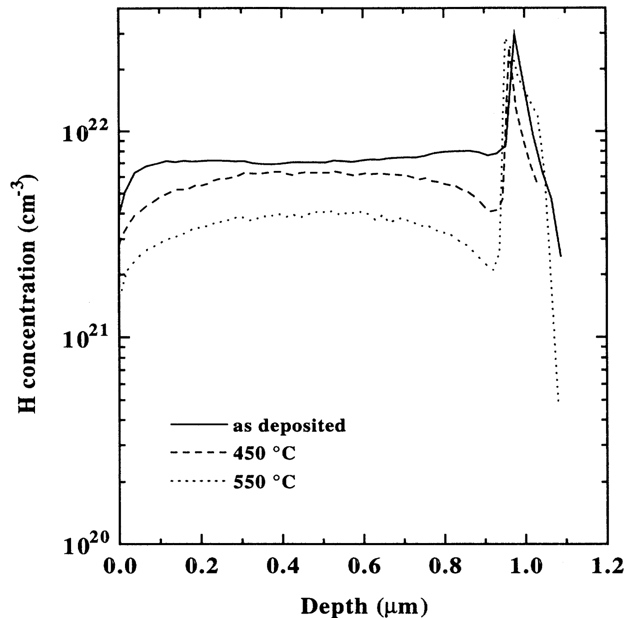

FIG. 4. Hydrogen depth profiles of as-deposited *a*-Si:H (solid curve) and after annealing at 450 (dashed curve) and 550 °C (dotted curve), respectively, for 1 h in the presence of monatomic H.

and dotted curves were obtained on specimens annealed at 450 and 550 °C for 1 h, respectively. The bulk H concentration decreases with increasing annealing temperature to 4×10^{21} cm^{-3} at 550 °C. At the sample surface (depth=0), however, the H loss is more pronounced. Although the specimens were annealed at temperatures at which solid-state crystallization usually occurs, the *a*-Si:H films did not crystallize. This presumably is due to the presence of monatomic H from the plasma which suppresses the motion of vacancies and interstitials.

The quenched specimens were characterized by measurements of the optical subband-gap absorption in the annealed state *A*, after annealing, and after intense light soaking (state *B*). The high-temperature anneals caused the photoconductivity to decrease by about 2–3 orders of magnitude, which is due to an enhanced loss of H at the surface (Fig. 4). This leads to a higher defect density at the sample surface, and thus increases the concentration of recombination centers in this region. The CPM spectra of the various states, normalized to the saturation value at $h\nu=2$ eV, are plotted in Fig. 5. The control sample is represented by the solid curves, and the dotted and dashed curves were obtained on specimens which were annealed at 450 and 550 °C, respectively. Figure 5(a) represents the annealed state *A*, and Fig. 5(b) shows the CPM spectra after prolonged illumination with white light. CPM spectra of the annealed samples do not exhibit an increase of the defect density due to the pronounced H loss at the sample surface, since the CPM technique is only sensitive to bulk defects. It is most striking that the high-temperature anneals did not affect the Urbach slope, which was found to be $E_T=48$ meV, indicating that the weak-bond distribution is not determined by a thermal equilibrium reaction with strong Si-Si bonds. Light soaking, on the other hand, still increases the defect density, and the change of N_D is plotted in the inset of Fig. 5(b) as a function of the annealing temperature T_A. While approximately the same number of defects are generated in the control sample and in the film annealed at 450 °C, the defect creation is less pronounced in the specimen annealed at 550 °C. Since the Urbach tail remained unchanged, the improved stability is most likely due to a loss of hydrogen in the bulk of the sample. This is consistent with the observation that high deposition temperatures reduce the light-induced defect creation in *a*-Si:H, which was attributed to a decrease of the hydrogen content.[3]

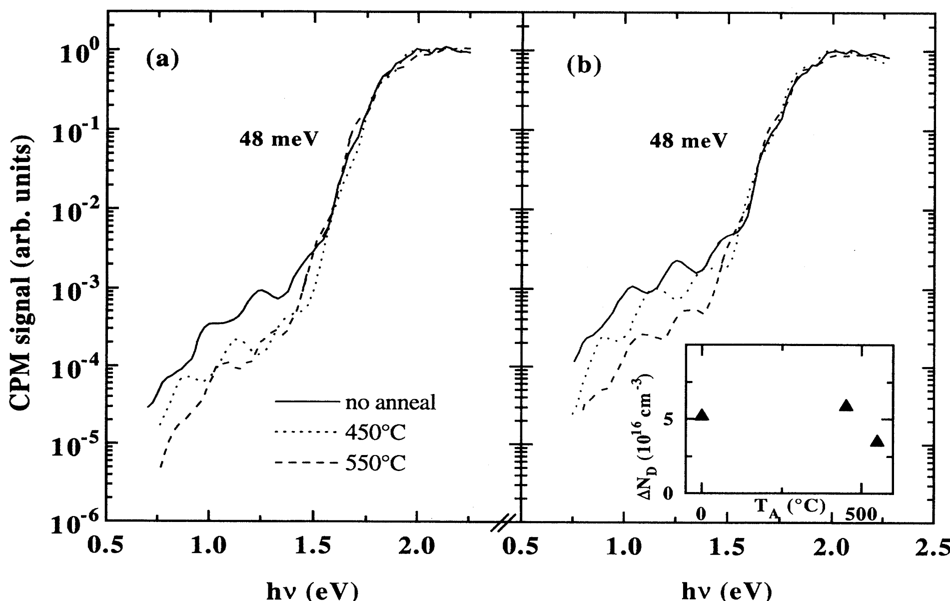

FIG. 5. Normalized CPM spectra of a *a*-Si:H films measured at 300 K. The solid curves represent the control sample. The dotted and dashed curves were obtained after annealing *a*-Si:H films at 450 and 550 °C, for 1 h, respectively. (a) State *A*; (b) after illumination with white light ($P=5$ W cm^{-2}) at 300 K for 15 h. The inset in (b) shows the change of the defect density, ΔN_D, as a function of the annealing temperature T_A.

IV. DISCUSSION

According to the results of Sec. III, the various properties of the material cannot be improved by posthydrogenation, annealing, or a combination of the two. The weak-bond concentration, metastability, and defect concentration do not change significantly. These results have a number of important implications for structure and H bonding of amorphous silicon discussed below.

A. Implications for hydrogen bonding

Exposure to monatomic hydrogen caused an increase of the total Si-H bond concentration by 3×10^{21} cm^{-3} and a decrease in half that number of Si-Si bonds. The density of resulting Si-H bonds exceeds the defect density by more than five orders of magnitude. The probability of breaking a Si-Si bond depends on the energies of breaking the bond and formation of Si-H bonds. Energetically favorable sites are the 10^{20}-cm^{-3} weak Si-Si bonds typically found in device-grade *a*-Si:H. An increase in H concentration should increase the Si-H concentration at the expense of the weak Si-Si concentration, allowing the amorphous network to relax. Expressed in terms of the hydrogen chemical potential, the increase in H concentration is expected to raise the hydrogen chemical potential from μ_H to μ_H^*. Thus the density of weak bonds would decrease and, consequently, the Urbach tail would steepen (dotted line in Fig. 6).[15] Although the added D concentration exceeds the weak-bond concentration by a factor of 30, the weak Si-Si bond distribution remains essentially unchanged (Fig. 2). Moreover, the incorporation of excess hydrogen does not cause the defect density to decrease. Thus the additional D atoms are accommodated at lattice sites where Si dangling bonds did not exist before or after the plasma exposure. These results require that hydrogen enters the sample in pairs. Each broken Si-Si must form two Si-H bonds with a very high probability. Therefore, once a Si-Si bond is broken, the probability of passivating both dangling bonds with hydrogen must be much greater than the probability of breaking a second Si-Si bond. This property has been explained in terms of a negative-U system for H in *a*-Si:H,[16] and can readily be accounted for by the formation of two hydrogen complexes such as H_2^* or larger paired H complexes (H_{2n}^*). In such a case, μ_H is pinned and appears to be very weakly dependent on the total H concentration.

This result can be tested using H evolution on thick samples where evolution is diffusion limited. In Fig. 7, the observed evolution of H from a thick sample (solid curve) is compared to the evolution expected if the diffusion activation energy remains constant (dashed curve) (constant chemical potential) or if the activation energy increases (dashed-dotted curve) (decreasing chemical potential) assuming a slowly varying density of states. The evolution expected from a layer was approximated using a finite state model. At any given time t_i, the state of the layer $S_i=(F_i,\mu_i,T_i,c_i,\theta_i)$ can be approximately characterized by the hydrogen flux F_i from the layer, the average hydrogen chemical potential μ_i, the temperature T_i, the average H concentration c_i, and the diffusion distance squared θ_i. Given these values at t_i it is possible to estimate the state of the layer S_{i+1} at a later time $t_{i+1}=t_i+\Delta t$, assuming a density of states, a model for the flux as a function of the other state variables, and the known variation of temperature with time. Further details are given in Ref. 17, where it is shown that the model is exact for diffusion from a layer with H bound at a single level, at very early times, and for times and temperatures such that $\theta > d^2$ where d is the layer thickness

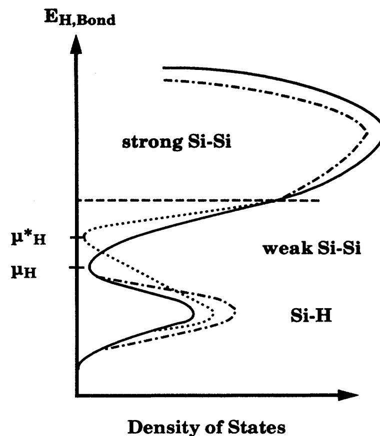

FIG. 6. Schematic spatial distribution for hydrogen in *a*-Si:H. Silicon-hydrogen bonds (Si-H) are located below the hydrogen chemical potential μ_H, while strong and weak Si-Si bonds are above μ_H. An increase of μ_H to μ_H^* decreases the weak-bond density, which results in a steeper Urbach tail (dotted line). The dashed-dotted line shows the change in the density of states if μ_H is pinned and all Si-Si bonds are removed with equal probability.

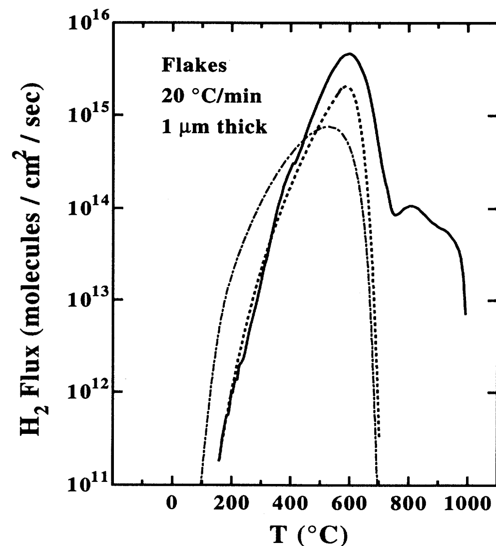

FIG. 7. Hydrogen evolution of 1-μm-thick *a*-Si:H as a function of the substrate temperature (solid curve). The dashed curve represents the expected evolution profile for a single concentration-independent diffusion activation energy, and the dashed-dotted curve shows the expected profile for an increasing diffusion activation energy.

when H is bound in a distribution of energy levels. The only place the model is expected to be approximate is on the low-temperature side of an evolution peak where there is a wide distribution of binding energies.

The observed narrow evolution peak (Fig. 7) is consistent with a diffusion activation energy that is independent of H content even after a significant portion of the H is evolved. Only well beyond the evolution peak after most of the H is evolved is there any indication that the evolution (and therefore the diffusion) is slowing down due to an increase in the activation energy. Therefore, the H chemical potential must remain independent of concentration over a large H concentration range; the chemical potential appears to be pinned for most H concentrations. This is consistent with the negative-U model of H and the idea that H forms Si-H bonds in pairs.

The experimentally observed pinning of the hydrogen chemical potential μ_H is indicative of a reversed order of the single and double occupied states for H in silicon placing the single occupancy configuration above μ_H and the zero and double occupancy states below μ_H.[16] H which diffuses into the sample and changes the occupation of a state from zero to one by breaking a strained or weak Si-Si bond creates an Si-H and leaves an unoccupied state (Si dangling bond) above μ_H which immediately will attract a second H. Hence the vast increase of the total H plus D concentration preferentially increases the number of doubly occupied sites which causes the defect density to remain unchanged (Fig. 2). On the other hand, one would assume that this would result in the passivation of preexisting weak Si-Si bonds. Since this is not the case the added H most likely decreases the strong-bond concentration, as depicted schematically in Fig. 6 (dashed-dotted line).

The concentration of H atoms bound to preexisting Si dangling bonds can be estimated from the high-temperature ($T > 700\,^{\circ}$C) evolution peak in Fig. 7, and amounts to a concentration of only $\sim 10^{19}-10^{20}$-cm^{-3} H atoms, while the majority of H atoms is accommodated with a binding energy of 1.4–1.7 eV (low-temperature peak in Fig. 7). Most likely these low-energy configurations are H_{2n}^{*} clusters rather than isolated H pairs for several reasons. First, the strain field associated with isolated H pairs would cause the network strain to increase roughly in proportion to the number of H pairs. For H_{2n}^{*} clusters, newly introduced hydrogen breaks perimeter strained Si-Si bonds which relax and distribute their strain energy to adjacent sites causing these bonds to weaken. Thus the overall strain energy and the concentration of strained bonds remain approximately constant, increasing only very slowly compared to the number of H atoms added. Second, the H binding energy of the average isolated H pair formed from strong Si-Si bonds is about 0.5 eV too small. Finally, the H_{2n}^{*} complex has been observed as an extended planar defect in single-crystalline silicon.[18,19] In *a*-Si:H the growth of clusters as large as in *c*-Si may be prevented because of the lack of a long-range order. H clusters nucleate and grow at H concentrations above 10^{20} cm^{-3}, pinning the chemical potential.[20] Thus the data lends further support to the idea the H clusters dominate H bonding in *a*-Si:H.

B. Creation and annihilation of lattice strain

Interesting connections between H bonding, network bonding, and exponential band edges can be derived from these results. From the data it is clear that neither the band-tail slopes nor the defect density appear to depend on temperature if the H content remains sufficiently high. Other data on annealing of unhydrogenated amorphized *c*-Si show that initially annealing reduces the network strain.[21] Once a minimum disorder is achieved, however, the exponential edges do not change significantly as a function of temperature or hydrogen concentration. This observation has two important consequences for the energetics of H bonding in amorphous silicon and metastable equilibrium of network strain.

First consider H bonding. If the network strain were in equilibrium, the disorder should increase as the temperature increases, causing a broadening of the exponential band tails. Furthermore, the network should crystallize if the network could sample all accessible states, since the crystalline state is clearly the lowest-energy state. However, neither result is observed. Annealing at temperatures below about 600 °C either with or without H does not result in further reduction in strain energy.[22] Figure 5 shows that increasing the temperature during hydrogenation does not increase the slope of the Urbach edge. These observations apparently indicate that the random network does not readily exchange strain energy with the rest of the system.

Experiments on recrystallization suggest that there is some sort of free-energy barrier to reaching lower-energy states such as crystallization or further large-scale reductions in strain energy. If *c*-Si is amorphized by self-implantation, the ensuing amorphous Si crystallizes only if the temperature is increased sufficiently high to overcome the free-energy barriers. Even at elevated temperatures, the material has a high probability of crystallizing from the substrate, which increases the likelihood of forming the appropriate configuration for crystallization. Thus, both our experiments as well as recrystallization of amorphized silicon suggest that the random network strain energy approaches a metastable equilibrium and *not* a thermal equilibrium.

However, we also expect that internal strains are more or less free to propagate within the network. A bond or group of bonds under compression or tension exert a force on neighboring atoms. Slight readjustments of these neighboring atoms in turn are transmitted further into the network. Small changes in atomic positions are therefore capable of propagating strains throughout the random network. Although the random network is not in thermal equilibrium, and it is not possible to reduce the total network strain below a certain minimum value, each bond distributes strain within the random network to its neighbors.

The following possible picture for network strain emerges. Starting with an unhydrogenated amorphous silicon-network produced at low temperatures, increased temperatures cause thermal motions which assist in propagating local internal strains throughout the network. Every so often, compressive and tensile local strains meet

and annihilate, thereby reducing the total silicon network strain. Similarly, introduction of H reduces the total network strain by removing the highly strained tensile bonds. Once a significant fraction of the strain has been removed either by annealing and/or hydrogenation, a quasi-steady-state situation is obtained. The rate of strain reduction is balanced by the rate of strain creation. For every tensile Si-Si bond eliminated by hydrogenation or annealing, a new one is created which is depicted schematically in Fig. 8 for the posthydrogenation. The average network strain and therefore the band edges remain independent of annealing or hydrogenation. A large free-energy barrier prevents the network from crystallizing in normal experimental time scales.

We can quantify the network strain during hydrogenation according to the following description. Let the total network strain energy E_{tot} varying in time according to

$$\frac{dE_{tot}}{dt}=R_{formation}(E_{tot})-R_{anneal}(E_{tot}) , \quad (1)$$

where $R_{formation}$ is the rate of strain-energy formation and R_{anneal} is the rate of strain-energy reduction. Both of the factors consist of a sum of thermal contributions as well as contributions due to H bonding and release. The experiments indicate that a steady state is achieved especially at temperatures between 400 and 600 °C. For thermal annealing, the rate of strain formation is related to the probability that an unstrained portion of the network thermally readjusts to create a pair of oppositely strained bonds which do not recombine but diffuse away. Examples include tensile and compressive pairs or oppositely bent bonds. The rate of strain reduction depends on the rate that oppositely strained bonds meet and recombine. R_{anneal} clearly depends on the strain diffusion rate and the concentration of mobile strained bonds. Because both thermal strain generation and annealing are expected to be highly temperature dependent, the lack of a temperature dependence means that the thermal generation and annealing is small compared to those strains involving H bonding and release.

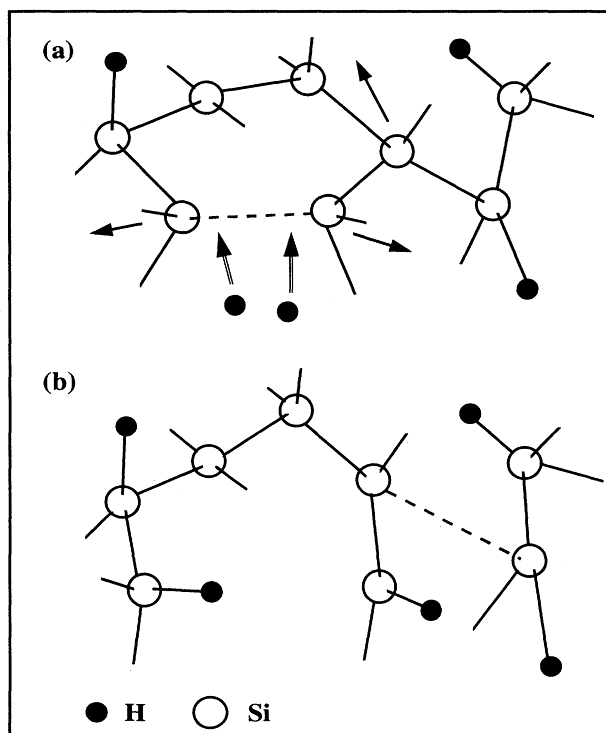

FIG. 8. Mechanism for the hydrogen-mediated reduction and creation of network strain. (a) Hydrogen from a plasma is introduced into *a*-Si:H. The lowest-energy site for the H incorporation is a weak Si-Si bond depicted by the dashed line. The tensile strain of this bond is reduced, and two Si-H bonds are formed (b). Breaking the weak bond allows the two Si atoms to relax, and accordingly strain propagates through the network to neighboring atoms, increasing their tensile stress (dashed line). The average network strain remains independent of the H concentration.

In the case of hydrogenation, H removes strained bonds through the formation of two Si-H bonds, and creates strain in order to accommodate the H in Si-H bonds. During hydrogenation or hydrogen evolution, the H bonding and release is governed by the reaction

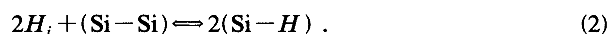

$$2H_i+(\mathrm{Si}-\mathrm{Si})\Longleftrightarrow 2(\mathrm{Si}-H) . \quad (2)$$

The change in total energy is given by

$$\Delta E_{tot}=2E_{\text{Si-H}}+(E_{network})_{after} -E_{\text{Si-Si}}-2E_{H_i}-(E_{network})_{before} , \quad (3)$$

where $E_{\text{Si-H}}$ and $E_{\text{Si-Si}}$ are the Si-H and Si-Si bond energies, respectively. If the Si-Si bond is a strained bond, we can write $E_{\text{Si-Si}}=E^0_{\text{Si-Si}}+E_{strain}$, where $E^0_{\text{Si-Si}}$ is the energy of a strong unstrained bond. Thus, each time the reaction occurs, there is a net change of total silicon-network strain energy of $\Delta E_{tot}=(E_{network})_{after}-E_{strain}-(E_{network})_{before}$. Because the net change in weak bonds appears to reach a steady state, $\Delta E_{tot}=0$, the average net change of energy for the H reaction reduces Eq. (3) to $2E_{\text{Si-H}}-E^0_{\text{Si-Si}}-2E_{\text{H}_i}$ for all Si-Si bonds even weak ones. Thus the H bonding is determined by the formation energy measured with respect to strong Si-Si bonds rather than weak bonds as is often assumed.

Given that during annealing and/or hydrogenation, network strain is being created and destroyed as the average strain decreases from some initial value to a final value, the question emerges concerning how a given network strain energy would be allocated among the various bonds since the bonds exchange strain energy. At first glance, the problem appears to be hopelessly underconstrained; we know only the total strain energy and are expected to determine the likely configuration of microscopic numbers of bonds. This problem is known to be solved using the principle of maximum entropy. If we assume that the total strain energy E_{tot} can be partitioned between the bonds in any number of ways which are all equally likely, then the most probable distribution of strain among the bonds is that distribution in which there are the most ways to obtain consistent with any constraints. Because entropy is the logarithm of the number of accessible states, the strain will maximize entropy sub-

ject to the constraints on the total network strain. This maximum entropy partition leads directly to exponential energy distributions for strain in the amorphous network.

Assume that the network consists of N bonds each of which can take strain energies E_j and $j=1,\ldots,M$ with probability P_j. The entropy is then given by

$$S=-N\sum_j P_j \ln(P_j) \; . \tag{4}$$

S is to be maximized with respect to P_j subject to the constraints that

$$\sum_j P_j=1 \; , \tag{5}$$

and that the total strain energy remains constant

$$E_{\text{tot}}=N\sum_j P_j E_j \; . \tag{6}$$

Using Lagrange multipliers, the probabilities can be solved for by maximizing the auxiliary function

$$\Omega=-N\sum_j P_j\ln(P_j)+\lambda\left[1-\sum_j P_j\right] +\beta\left[E_{\text{tot}}-N\sum_j P_j E_j\right] \; , \tag{7}$$

where the Lagrange multipliers λ and β are also determined by maximizing Ω. Taking partial derivatives and setting them equal to zero yields the following results:

$$P_j=\frac{\exp(-\beta E_j)}{\sum_j \exp(-\beta E_j)}=\frac{\exp(-\beta E_j)}{Z(\beta)} \; , \tag{8}$$

where β is given by

$$E_{\text{tot}}=-N\frac{\partial}{\partial\beta}\ln(Z(\beta)) \; . \tag{9}$$

We see that the probability that a bond has an energy E_j is exponential in the bond energy. If there are a large number of possible energies E_j, we can define a density of states $g(E)$ for the possible bond energies. While the density of states of possible strain-energy distributions $g(E)$ can have any kind of possible shape such as Gaussian, etc., the distribution of realized bond energies $g(E)\times p(E)$ will be dominated by the exponential $p(E)$ if $g(E)$ is broad compared to β. The strain bonds will be exponentially distributed with an exponential slope given by β. β has a direct physical interpretation from the above equations. β is approximately equal to E_{tot}/N when $E_{\text{tot}}/N<E_{\max}$, where the maximum energy $E_{\max}$ is given by $E_{\max}=\max_j(E_j)$. Thus we arrive at the important result that if the strain energy of the lattice is distributed around the lattice, the bonds are exponential in energy and the temperature is the average strain energy per bond (E_{tot}/N).

Assuming that the distribution of Si-Si bond energies can be identified with the Urbach edge, perhaps through a constant such as a deformation potential, a simple explanation for the Urbach tail often observed in amorphous materials is therefore obtained. Namely, the strain energy of the network is distributed among the bonds in the most probable configuration which requires that the bond energies occur with a probability exponential in the bond energy. The often observed Urbach slope is, to within a constant, related to the average strain per bond.

This result is consistent with scanning calorimetry measurements. The heat of crystallization of relaxed amorphous silicon is determined to be about 100 meV per Si atom for *c*-Si amorphized by self-implantation.[21] Since there are two bonds per Si atom, this suggests that the average strain energy per bond is around 50 meV. Furthermore, unrelaxed *a*-Si has an average strain of about 150–160 meV per atom or 75–80 meV per bond. According to the above discussion, this should be approximately the slope of the exponential silicon bond energy distribution. If there is a one-to-one correspondence between the electronic state energies and the bond energies, then the Urbach slope should be about 50 meV for relaxed *a*-Si and 75–80 meV for unrelaxed *a*-Si. Both these results are in approximate agreement with experimental data. The Urbach edge for *a*-Si:H is about 50 meV, and for unhydrogenated *a*-Si or *a*-Si with H evolved it is about 100 meV. Thus calorimetry observations confirm the idea that the Urbach slope represents the average strain energy per bond and the distribution of strain energy according to maximum entropy. These ideas are probably worth further investigation.

V. SUMMARY

Exposing device-grade *a*-Si:H films to monatomic D from a remote plasma, we increased the total hydrogen concentration by 3×10^{21} cm^{-3}. According to Raman-backscattering measurements the added deuterium was bound to silicon. This vast increase of the total Si-H/Si-D concentration neither caused the defect density to decrease, the Urbach tail to steepen, nor the amorphous network to stabilize. These results are incompatible with a simple trap-filling model. However, they support the idea of a negative correlation energy for H and/or D in silicon and are consistent with a model in which H is trapped and released from hydrogen clusters which nucleate and grow in response to added H.[20] High-temperature annealing also does not affect the defect density or the Urbach tail, suggesting that the network strain energy is in metastable equilibrium and *not* in thermal equilibrium. Once the strain energy reaches a minimum by either hydrogenation or annealing, a steady state between strain reduction and creation is obtained. Existing strain is distributed in the network according to maximum entropy, which gives rise to exponential band tails. Furthermore, we suggest that the Urbach slope, characteristic of amorphous semiconductors, represents to within a constant the average strain energy per network bond.

ACKNOWLEDGMENTS

This work was supported by NREL. One of the authors (N.H.N.) is pleased to acknowledge partial support from the Alexander von Humboldt Foundation, Federal Republic of Germany.

[1]H. Dersch, J. Stuke, and J. Beichler, Appl. Phys. Lett. **38**, 456 (1980).

[2]N. H. Nickel, W. B. Jackson, and N. M. Johnson, Phys. Rev. Lett. **71**, 2733 (1993).

[3]A. H. Mahan, and M. Vanececk, *Amorphous Silicon Materials and Solar Cells,* edited by B. L. Stafford, AIP Conf. Proc. No. 234 (American Institute of Physics, New York, 1991), Vol. 234, p. 195.

[4]N. M. Johnson, C. E. Nebel, P. V. Santos, W. B. Jackson, R. A. Street, K. S. Stevens, and J. Walker, Appl. Phys. Lett. **59**, 1443 (1991).

[5]J. Kakalios and R. A. Street, Phys. Rev. B **34**, 6014 (1986).

[6]N. M. Johnson, J. Walker, and K. W. Stevens, J. Appl. Phys. **69**, 2631 (1991).

[7]B. Tuck, *Introduction to Diffusion in Semiconductors* (Peregrinus, Salisbury, 1974).

[8]P. V. Santos and W. B. Jackson, Phys. Rev. B **46**, 4595 (1992).

[9]J. B. Boyce, N. M. Johnson, S. E. Ready, and J. Walker, Phys. Rev. B **46**, 4308 (1992).

[10]L. Ley, in *Semiconductors and Semimetals, Hydrogenated Amorphous Silicon,* edited by J. I. Pankove (Academic, San Diego, 1984), Vol. 21, Chap. 12.

[11]I. An, Y. M. Li, C. R. Wronski, H. V. Nguyen, and C. R. Collins, Appl. Phys. Lett. **59**, 2543 (1991).

[12]Y. M. Li, I. An, M. Gunes, R. M. Dawson, R. W. Collins, and C. R. Wronski, in *Amorphous Silicon Technology,* edited by M. J. Thompson, Y. Hamakawa, P. G. LeComber, A. Modan, and E. A. Schiff, MRS Symposia Proceedings No. 258 (Materials Research Society, Pittsburgh, 1992), p. 57.

[13]J. S. Williams, in *Beam-Solid Interactions and Phase Transformations,* edited by H. Kurz, G. L. Olson, and J. M. Poate, MRS Symposia Proceedings No. 51 (Materials Research Society, Pittsburgh, 1985), p. 851.

[14]G. L. Olsen, S. A. Kokorowski, J. A. Roth, and L. D. Hess, in *Laser-Solid Interactions and Transient Thermal of Materials,* edited by J. Narayan, W. L. Brown, and R. A. Lemons, MRS Symposia Proceedings No. 13 (Materials Research Society, Pittsburgh, 1983), p. 141.

[15]R. A. Street, Phys. Rev. B **43**, 2454 (1991).

[16]S. Zafar and E. A. Schiff, Phys. Rev. B **40**, 5235 (1989).

[17]W. B. Jackson and N. H. Nickel (unpublished).

[18]N. M. Johnson, F. A. Ponce, R. A. Street, and R. J. Nemanich, Phys. Rev. B **35**, 4166 (1987).

[19]W. B. Jackson and S. B. Zhang, Physica B **170**, 197 (1991).

[20]W. B. Jackson, P. V. Santos, and C. C. Tsai, Phys. Rev. B **47**, 9993 (1993).

[21]S. Roorda, S. Doorn, W. C. Sinke, P. M. L. O. Scholte, and E. Van Lorenen, Phys. Rev. Lett. **62**, 1880 (1989).

[22]S. Roorda, Ph.D. thesis, Utrecht, The Netherlands, 1990.